Clinical Radiology 74 (2019) 734.e7–734.e12

Contents lists available at ScienceDirect

Clinical Radiology

journal homepage: www.clinicalradiologyonline.net

Efficacy of PROPELLER in reducing ocular motion artefacts and improving image quality of orbital MRI at 3 T using an eye surface coil

H. Jiang [a,b], S. Wang [a,b], J. Xian [a,b,*], Q. Chen [a,b], W. Wei [b,c]

[a] Department of Radiology, Beijing Tongren Hospital, Capital Medical University, Beijing 100730, China
[b] Clinical Center for Eye Tumors, Capital Medical University, Beijing 100730, China
[c] Beijing Tongren Eye Center, Beijing Tongren Hospital, Capital Medical University, Beijing 100730, China

ARTICLE INFORMATION

Article history:
Received 9 January 2019
Accepted 20 May 2019

AIM: To evaluate the efficacy of periodically rotated overlapping parallel lines with enhanced reconstruction (PROPELLER) in reducing ocular motion artefacts and improving image quality of orbital magnetic resonance imaging (MRI) at 3 T using an eye surface coil.

MATERIALS AND METHODS: Forty-six patients underwent orbital 3 T MRI using an eye surface coil. The pre-contrast axial T2-wighted (W) PROPELLER and T1 fluid-attenuated inversion recovery (FLAIR) PROPELLER imaging were performed on 21 patients, and conventional T2W and T1W imaging were performed on 25 patients. The ocular motion artefacts, delineation of anatomical structures, depiction of lesions, and image quality were evaluated independently by two radiologists using a five-point scale. The signal-to-noise ratios (SNRs) of anatomical structures and lesions were measured.

RESULTS: The interobserver agreement was good to excellent (kappa values from 0.79 to 0.91). PROPELLER sequences had higher scoring than the conventional sequences in all cases ($p<0.05$). PROPELLER images showed fewer motion artefacts, higher image quality, and more clear delineation of anatomical structures and lesions than the non-PROPELLER images. T2W PROPELLER images produced higher SNRs in lens, vitreous body, lacrimal gland, and lesions than conventional T2W images ($p<0.05$). T1 FLAIR PROPELLER images showed lower SNRs in lens, vitreous body, medial rectus, lateral rectus, temporalis, and posterior half of optic nerve than conventional T1W images ($p<0.05$).

CONCLUSION: PROPELLER can effectively reduce ocular motion artefacts and improve image quality, which plays an important role in clearly delineating anatomical structures and lesions on orbital 3 T MRI using an eye surface coil.

Introduction

Three tesla magnetic resonance imaging (MRI) plays a critical role in depicting anatomical details and pathological abnormalities in the orbit, especially with high-resolution eye surface coils[1,2]; however, the eye surface coils increase

* Guarantor and correspondent: Junfang Xian, Department of Radiology, Beijing Tongren Hospital, Capital Medical University, Beijing 100730, China.
E-mail address: cjr.xianjunfang@vip.163.com (J. Xian).

https://doi.org/10.1016/j.crad.2019.05.014
0009-9260/

the susceptibility of involuntary ocular movement, which leads to significant motion artefacts and degrades the image quality.[2–5] Therefore, high-quality images are required for superior visibility of detailed anatomical structures and lesions in the orbit.

The cued blinking protocol has been proven successful to eliminate ocular movement artefacts during MRI, but some patients fail to adhere to the cued blinking instructions.[4] The dual-source parallel transmission 3D sequence has been used to hasten acquisition and reduce motion artefacts; however, the signal-to-noise ratios (SNRs) were too low compared to conventional MRI.[6] Moreover, fast T1 or T2-weighted imaging (WI) is frequently used to reduce the scanning time that patients must hold the eyeball motionless; however, this results in decreased image quality.[2]

Recently, the periodically rotated overlapping parallel lines with enhanced reconstruction (PROPELLER) sequence has been widely used in brain, head and neck, abdomen, and knee MRI.[7–15] This is a technique developed to reduce motion artefacts with radial k-space coverage, and can be used with other sequences, such as fast spin-echo (FSE) and fast-recovery FSE (FRFSE), for motion correction, and it yields a high SNR.[9,16,17] The FSE T2W PROPELLER technique has been used in internal auditory canal imaging, which reduces motion artefacts and improves image quality.[9] FSE T1 fluid attenuated inversion recovery (FLAIR) PROPELLER imaging has been reported to improve visualisation of anatomical structures and lesions in the brain.[15] Nevertheless, there is no report regarding the application of PROPELLER in orbital MRI to the authors' knowledge. Therefore, the aim of this study was to investigate the efficacy of PROPELLER in reducing ocular motion artefacts and improving image quality on 3 T MRI of orbit using an eye surface coil.

Materials and methods

Study population

This prospective study was approved by the institution's ethics committee. Written informed consent for participation in this study was signed by all participants. From January 2018 to June 2018, 50 consecutive patients clinically suspected of eye disease were recruited. Four patients were excluded because of contraindications to MRI. Finally, a total of 46 patients (age, 26–73 years; mean age, 48.1 years) including 13 men (age, 28–70 years; mean age, 42.5 years) and 33 women (age, 26–73 years; mean age, 56.1 years) were included. The general features of patients with eye lesions are presented in Table 1.

MRI protocol

All examinations were performed using a 3 T MRI system (Discovery MR750, General Electric, Milwaukee, WI, USA), with an eight-channel phased-array eye surface coil (Medcoil EYE80, Suzhou Medcoil Healthcare, China). Twenty-one patients were randomly selected to acquire pre-contrast axial images with PROPELLER, and 25 patients without PROPELLER. FRFSE T2W PROPELLER and FSE T1 FLAIR PROPELLER imaging were performed in the PROPELLER group, and conventional FRFSE T2W and FSE T1W imaging were performed in the non-PROPELLER group. Imaging protocols are listed in Table 2. Patients were asked to keep their eyes closed and as relaxed as possible during image acquisition and all patients were able to comply with this request. The post-contrast T1W images were obtained with two-point Dixon fat/water separation (FLEX) in all 46 patients, and PROPELLER was not used.

Table 1
General features of patients with eye lesions.

Eye lesions	No.	Sex		Age
		Male	Female	
Intra-ocular mass	13	5	8	52.1±4.6
Orbital mass	10	4	6	48.5±3.5
Dacryoadenitis	15	3	12	43.9±6.1
Graves ophthalmopathy	6	1	5	55.4±8.6
Optic neuropathy	2	0	2	43.6±7.9
Total	46	13	33	48.1± 5.2

Data are the mean±standard deviation.

Imaging analysis

All the pre-contrast MRI data, including PROPELLER and non-PROPELLER images were analysed. The lesions and critical anatomical structures were assessed (Table 3). Two experienced radiologists independently evaluated ocular motion artefacts and depiction of anatomical structures in each patient using a picture archiving and communication system (Huahai, version 3.0; Huahai Medical Info-tech, China). They were blinded to subject data and MRI acquisition conditions. A five-point grading scale (0 = extremely severe artefacts, unacceptable depiction and non-diagnostic image quality; 1 = severe artefacts, poor depiction and image quality; 2 = moderate artefacts and depiction, fair image quality; 3 = mild artefacts, clear depiction and good image quality; and 4 = no artefacts, excellent depiction and image quality) was used to evaluate ocular motion artefacts and image quality. The subjective score graded by the two observers was averaged.

Table 2
Imaging parameters for PROPELLER and non-PROPELLER imaging.

Parameters	PROPELLER		Non- PROPELLER	
	FRFSE T2W	FSE T1 FLAIR	FRFSE T2W	FSE T1W
FOV (cm)	12	12	12	12
TR (ms)	3000	2232	3000	591
TE (ms)	95	45	95	8
Thickness/gap (mm)	3/0.3	3/0.3	3/0.3	3/0.3
Matrix	384×384	384×384	384×384	384×384
BW (kHz)	83.3	125	41.7	50
ETL	26	16	21	3
NEX	2	2.5	4	4
Scanning time (min: s)	1: 36	2: 18	2: 06	2: 46

FOV, field of view; TR, repetition time; TE, echo time; BW, bandwidth; ETL, echo train length; NEX, number of excitations.

Table 3
Imaging assessment for critical anatomical structures in orbit.

Anatomical structures	Subjective assessment	Objective assessment
Eyeball	Sclera, retinal choroid complex, ciliary body, iris, lens	Lens, vitreous body (anterior and posterior half)
Extraocular muscles	Medial rectus muscle, medial rectus muscle insertion, lateral rectus muscle, lateral rectus muscle insertion	Medial rectus muscle (anterior and posterior half), lateral rectus muscle (anterior and posterior half)
Temporalis	Temporalis	Temporalis
Optic nerve and vessel	Optic nerve, superior ophthalmic vein	Optic nerve (anterior and posterior half)
Lacrimal gland	Lacrimal gland	Lacrimal gland
Orbital septum	Orbital septum	None

Objective image analysis was performed on a GE AW 4.6 workstation (GE Healthcare). An experienced radiologist measured the following metrics: (a) signal intensity values of anatomical structures and lesions in orbit (SI_{orbit}), and (b) the standard deviation of the background noise (SD_{noise}) for each image. The size of region of interest (ROI) used for the anatomical structures was 2 mm^2, for the orbital lesion was 10 mm^2, avoiding necrotic foci or vessels. The SD_{noise} was measured at a circular ROI of 2 mm^2, and the ROI was positioned in an area anterior to the orbit. The SNR was calculated according to the following formula[18]: $SNR = SI_{orbit} / SD_{noise}$. SNR was measured twice and averaged.

Statistical analysis

All statistical analyses were performed with SPSS 17.0 (SPSS, Chicago, IL, USA) software. Wilcoxon's signed rank test was used to compare the average score between the PROPELLER and non-PROPELLER images. Agreement in scoring between the two observers was assessed with the weighted Cohen's kappa test. The kappa values were interpreted as: <0.40, poor; 0.41–0.60, moderate; 0.61–0.80, good; and >0.81, excellent. To avoid the bias arising from the interaction between left and right eye movements, the generalised estimating equation, introduced by Zeger *et al.*,[19] was applied to compare the differences in SNRs between PROPELLER and non-PROPELLER images. $p<0.05$ was considered to indicate a significant difference.

Results

Subjective image quality assessment

The results of subjective assessment from all the patients are presented in Table 4. In all the comparisons, the PROPELLER sequence had a higher scoring than the conventional sequence with the differences being statistically significant ($p=0.000$). More specifically, T2W and T1 FLAIR images obtained with PROPELLER showed fewer ocular motion artefacts and higher image quality than the images obtained without PROPELLER. The anatomical structures and lesions in orbit were depicted more clearly on PROPELLER images than those on non-PROPELLER images (Figs 1 and 2). Agreement between the two independent observers was good to excellent with kappa values ranging between 0.79 and 0.91 (Table 4).

Objective image quality assessment

The differences in SNRs between PROPELLER and non-PROPELLER images are presented in Tables 5 and 6. The T2W images obtained with PROPELLER showed higher SNRs in lens, vitreous body, lacrimal gland, and lesions than the T2W images without PROPELLER ($p<0.05$). There were no

Table 4
Scores and interobserver agreement for subjective assessment.

Anatomical structures and lesions	T2W		T1W		*p*-Value	*k*-Value
	PROPELLER	Non-PROPELLER	PROPELLER	Non-PROPELLER		
Sclera	3.61±0.22	2.21±0.49	3.67±0.46	2.43±0.78	0.000	0.90
Retinal choroid complex	3.77±0.42	2.25±0.32	3.85±0.34	2.13±0.47	0.000	0.88
Ciliary body	3.81±0.40	2.31±0.18	3.66±0.22	2.65±0.27	0.000	0.83
Iris	3.98±0.03	2.66±0.45	3.87±0.53	2.23±0.82	0.000	0.88
Lens	3.83±0.24	2.24±0.14	3.76±0.17	2.13±0.42	0.000	0.91
Medial rectus muscle	3.81±0.40	2.53±0.51	3.82±0.39	2.76±0.74	0.000	0.80
Medial rectus muscle insertion	3.54±0.12	2.09±0.17	3.39±0.09	2.17±0.64	0.000	0.82
Lateral rectus muscle	3.85±0.33	2.19±0.36	3.80±0.27	2.06±0.28	0.000	0.89
Lateral rectus muscle insertion	3.56±0.11	2.03±0.51	3.32±0.31	2.20±0.16	0.000	0.79
Temporalis	3.61±0.22	2.43±0.56	3.69±0.32	2.33±0.72	0.000	0.79
Optic nerve	3.79±0.40	2.53±0.49	3.80±0.41	2.75±0.76	0.000	0.90
Superior ophthalmic vein	3.66±0.28	2.24±0.28	3.72±0.63	2.64±0.55	0.000	0.81
Lacrimal gland	3.77±0.42	2.53±0.51	3.79±0.41	2.73±0.78	0.000	0.86
Orbital septum	3.77±0.42	2.53±0.51	3.79±0.41	2.69±0.85	0.000	0.83
Lesions	3.79±0.40	2.50±0.51	3.83±0.38	2.72±0.83	0.000	0.88

Data are the mean ± standard deviation.

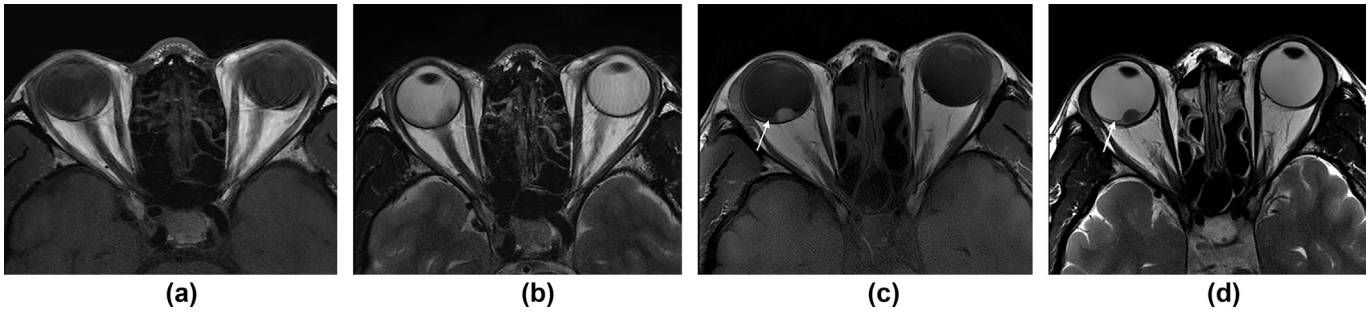

Figure 1 (a, b) A 35-year-old woman with a right intra-ocular mass. Severe motion artefacts from involuntary ocular movements degrade conventional (a) T1W and (b) T2W images. The mass and adjacent critical anatomical details are obscured by ocular motion artefacts. (c, d) A 47-year-old woman with a right intra-ocular mass. (c) T1 FLAIR and (d) T2W PROPELLER images show no ocular motion artefacts, the mass and adjacent anatomical details are clearly depicted. The detached retina around the mass is clearly visible on both images (arrow).

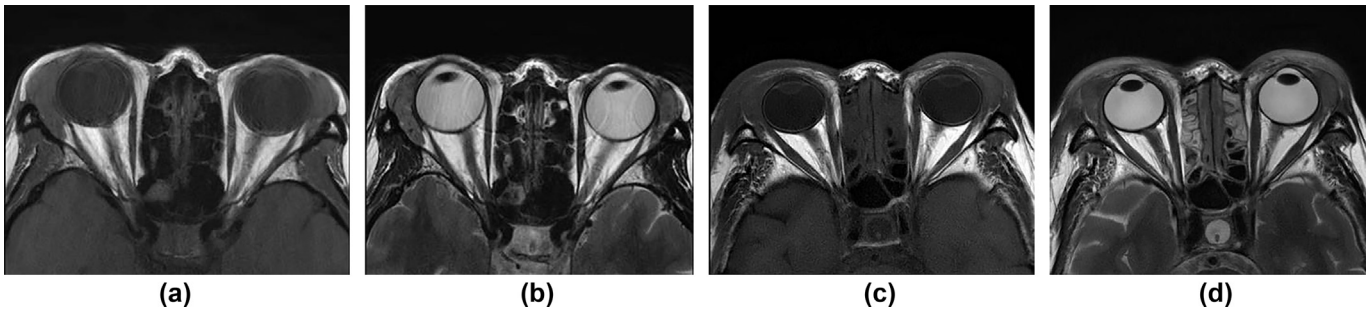

Figure 2 (a, b) A 44-year-old man with bilateral dacryoadenitis. Conventional (a) T1W and (b) T2W images show severe motion artefacts propagated along the horizontal axis, decreasing the image quality. (c, d) A 36-year-old woman with bilateral dacryoadenitis. (c) T1 FLAIR and (d) T2W PROPELLER images show no ocular motion artefacts, the enlarged lacrimal glands and oedematous eyelids are clearly visualised.

Table 5
Objective assessment of T2W imaging with and without PROPELLER.

Anatomical structures and lesions	PROPELLER	Non-PROPELLER	Standard deviation	*p*-Value
Lens	3.95±1.67	2.17±2.14	0.047	0.005
Anterior half of vitreous body	80.74±24.12	51.33±18.62	0.000	0.003
Posterior half of vitreous body	67.39±22.01	48.40±16.82	0.037	0.000
Anterior half of medial rectus	5.55±2.10	6.03±3.65	0.035	0.573
Posterior half of medial rectus	5.82±2.38	5.74±2.54	0.020	0.889
Anterior half of lateral rectus	5.80±4.09	5.22±2.42	0.000	0.529
Posterior half of lateral rectus	6.98±3.99	5.45±2.66	0.083	0.073
Temporalis	5.38±2.66	5.02±0.09	0.066	0.589
Anterior half of optic nerve	11.84±6.43	10.00±3.04	0.048	0.587
Posterior half of optic nerve	7.96±3.13	6.43±1.97	0.068	0.059
Lacrimal gland	14.67±4.79	9.80±5.76	0.020	0.008
Lesions	19.58±5.46	10.88±3.85	0.001	0.000

Data are the mean ± standard deviation.

significant differences in SNRs of medial rectus, lateral rectus, temporalis, and optic nerve between T2W images with and without PROPELLER ($p>0.05$).

The T1 FLAIR images acquired with PROPELLER showed lower SNRs in lens, vitreous body, medial rectus, lateral rectus, temporalis, and posterior half of optic nerve compared to the T1W images without PROPELLER ($p<0.05$). No significant differences were found in SNRs of anterior half of optic nerve, lacrimal gland, and lesions between PROPELLER and non-PROPELLER images ($p>0.05$).

Discussion

In the present study, the orbital PROPELLER images showed fewer ocular motion artefacts, higher overall image quality, and clearer visibility of anatomical structures and lesions compared to non-PROPELLER images. These findings were similar to those reported in previous PROPELLER MRI studies in head and neck, shoulder, abdomen, and knee.[10–14,17] These might be caused by the excellent performance on reduction of motion artefacts for

Table 6
Objective assessment of T1W imaging with and without PROPELLER.

Anatomical structures and lesions	PROPELLER	Non-PROPELLER	Standard deviation	*p*- Value
Lens	12.77±3.45	21.97±6.63	0.027	0.001
Anterior half of vitreous body	9.83±2.84	16.02±4.22	0.077	0.000
Posterior half of vitreous body	8.13±2.48	11.33±2.85	0.059	0.000
Anterior half of medial rectus	6.05±2.87	11.59±3.28	0.005	0.000
Posterior half of medial rectus	5.17±2.34	9.20±3.05	0.000	0.000
Anterior half of lateral rectus	5.39±4.12	10.50±5.42	0.000	0.007
Posterior half of lateral rectus	5.59±2.71	9.61±4.79	0.081	0.000
Temporalis	9.91±4.37	15.28±7.78	0.004	0.021
Anterior half of optic nerve	9.63±5.02	10.31±5.31	0.028	0.195
Posterior half of optic nerve	7.51±2.59	10.57±2.98	0.078	0.016
Lacrimal gland	15.74±7.19	17.84±8.39	0.003	0.352
Lesions	15.17±8.38	17.08±7.79	0.001	0.214

Data are the mean ± standard deviation.

PROPELLER.[4,10–14,17] The PROPELLER sequence is a radial k-space sampling concept, and the k-space acquisition scheme with rotating, partially overlapping “blades” is beneficial for reducing motion artefacts during data sampling because the central region of the k-space is sampled at multiple times.[20–22] In PROPELLER imaging, the number of blades needs to sufficiently cover the k-space, and increasing blade coverage leads to improvement in motion correction effects but also the image quality.[9,20–22]

T2W PROPELLER imaging has been reported to not only reduce motion artefacts but also contribute to better SNR.[7,9,12,23] The present objective results showed that T2W PROPELLER imaging produced higher SNRs in the lens, vitreous body, lacrimal glands and lesions than the non-PROPELLER imaging; however, no difference was found in other anatomical structures. The SNR is affected by various factors, and similar parameters were selected in T2W PROPELLER and non-PROPELLER imaging. Therefore, the differences in SNRs may be caused by the characteristics of orbital anatomy and PROPELLER technique.

Motion artefacts are often more produced in the anterior part of the eyes, as with a small change in gaze direction, the lens and vitreous body move quite significantly, while other structures, such as the optic nerve and extraocular muscles remain in the same place. The lacrimal glands are fixed to the orbital periosteum, so produce few motion artefacts; however, ocular motion artefacts are propagated in the phase-encoding direction along the horizontal axis, which may affect the SNR measurements of lacrimal glands. In the present study, the majority of lesions, including intra-ocular masses and dacryoadenitis (28 lesions, 60.9%), were located in the anterior part of the orbit, which might make them susceptible to ocular motion. The PROPELLER technique is suitable for imaging moving objects due to its inherent ability to reject some of the in-plane as well as through-plane motion and its inherent averaging of the remaining data inconsistencies, which reduces the motion artefacts caused by involuntary movements.[9,23,24] Therefore, the significant increases in SNRs are considered to be due to the reduction of ocular motion artefacts by using PROPELLER.

The PROPELLER technique can be applied to T1 FLAIR sequence at 3 T, and the T1 FLAIR PROPELLER imaging has been used to improve the visualisation of anatomical structures and lesions.[15,24] The present objective results showed that T1 FLAIR PROPELLER imaging resulted in lower SNRs in the majority of orbital structures than the non-PROPELLER imaging, which was similar to previous studies.[24,25] FLAIR is a special inversion recovery sequence providing superior image contrast; however, the inversion pulses may lower the image SNR.[24,25] Moreover, the trade-off between motion correction performance and T1 contrast could explain the simultaneous reduction of motion artefacts and SNRs.[15] It is known that FSE-based acquisition for T1 FLAIR imaging is routinely used in the clinical setting with short echo train lengths (ETLs) to provide a high T1 contrast. To date, the PROPELLER with parallel imaging methods have typically used relatively long ETLs, which is the most effective approach to achieve wider blades to acquire motion-insensitive high-quality PROPELLER images. Therefore, the increases of ETLs result in lower SNRs in T1 FLAIR PROPELLER imaging. Although the T1W non-PROPELLER images had higher SNRs, the T1 FLAIR PROPELLER images had fewer ocular motion artefacts and higher overall image quality, which provided more clear delineation of anatomical details and pathological abnormalities of orbit.

The present study had several limitations. First, only the ocular motion artefacts were evaluated, other artefacts, including streak artefacts and susceptibility artefacts, were not assessed. Shimamoto *et al.* reported that streak artefacts had little influence on overall image quality.[26] The FSE sequence was used in the present study, which would minimise the susceptibility artefacts. Moreover, there were no significant differences between PROPELLER and non-PROPELLER images in terms of susceptibility artefacts.[26] Second, T1 FLAIR PROPELLER and conventional T1W imaging were compared in the present study, and there was a trade-off between motion correction capabilities and T1 contrast. Therefore, a novel technique should be explored to increase the overall blade width for motion correction while maintaining short echo trains to maintain desirable image contrast for T1W PROPELLER imaging. Third, the post-contrast T1W FLEX images were obtained without PROPELLER, which was because PROPELLER cannot be applied to the T1W fat suppression sequence at present. Fourth, PROPELLER combined with other sequences was not evaluated; however, this will be examined in future work.

In conclusion, the present study demonstrates that the PROPELLER technique can significantly reduce ocular motion artefacts and improve image quality, which is useful in clearly delineating anatomical details and lesions in the orbit using 3 T MRI with an eye surface coil.

Conflict of interest

The authors declare no conflict of interest.

Acknowledgements

The authors acknowledge the support of Beijing Municipal Administration of Hospitals Clinical Medicine Development of Special Funding Support (grant no. ZYLX201704) and high levels of health technical personnel in Beijing city (grant no. 2014-2-005).

References

1. Duong TQ. Magnetic resonance imaging of the retina: from mice to men. *Magn Reson Med* 2014;**71**(4):1526–30.
2. Christoforidid JB, Wassenaar PA, Christoforidis GA, *et al*. Retrobulbar vasculature using 7-T magnetic resonance imaging with dedicated eye surface coil. *Graefes Arch Clin Exp Ophthalmol* 2013;**251**(1):271–7.
3. Herrick RC, Hayman LA, Taber KH, *et al*. Artefacts and pitfalls in MR imaging of the orbit: a clinical review. *RadioGraphics* 1997;**17**(3):707–24.
4. Beenakker JWM, van Rijn GA, Luyten GPM, *et al*. High-resolution MRI of uveal melanoma using a microcoil phased array at 7 T. *NMR Biomed* 2013;**26**(12):1864–9.
5. Bittersohl B, Huang T, Schneider E, *et al*. High-resolution MRI of the triangular fibrocartilage complex (TFCC) at 3 T: comparison of surface coil and volume coil. *J Magn Reson Imaging* 2007;**26**(3):701–7.
6. Seeger A, Schulze M, Schuettauf F, *et al*. Feasibility and evaluation of dual-source transmit 3D imaging of the orbits: comparison to high-resolution conventional MRI at 3 T. *Eur J Radiol* 2015;**84**(6):1150–8.
7. Nagatomo K, Yabuuchi H, Yamasaki Y, *et al*. Efficacy of periodically rotated overlapping parallel lines with enhanced reconstruction (PROPELLER) for shoulder magnetic resonance (MR) imaging. *Eur J Radiol* 2016;**85**(10):1735–43.
8. Chen X, Xian J, Wang X, *et al*. Role of periodically rotated overlapping parallel lines with enhanced reconstruction diffusion-weighted imaging in correcting distortion and evaluating head and neck masses using 3 T MRI. *Clin Radiol* 2014;**69**(4):403–9.
9. Wu HB, Yuan HS, Ma F, *et al*. Comparison of FSE T2W PROPELLER and 3D-FIESTA of 3 T MR for the internal auditory canal. *Clin Imaging* 2017;**45**:30–3.
10. Ohgiya Y, Suyama J, Seino N, *et al*. MRI of the neck at 3 tesla using the periodically rotated overlapping parallel lines with enhanced reconstruction (PROPELLER) (BLADE) sequence compared with T2-weighted fast spin-echo sequence. *J Magn Reson Imaging* 2010;**32**(5):1061–7.
11. Lee JH, Choi YH, Cheon JE, *et al*. Improved abdominal MRI in non-breath-holding children using a radial k-space sampling technique. *Pediatr Radiol* 2015;**45**(6):840–6.
12. Hirokawa Y, Isoda H, Maetani YS, *et al*. Hepatic Lesions: improved image quality and detection with the periodically rotated overlapping parallel lines with enhanced reconstruction technique-evaluation of SPIO-enhanced T2-weighted MR images. *Radiology* 2009;**251**(2):388–97.
13. Lavdas E, Mavroidis P, Hatzigeorgiou V, *et al*. Elimination of motion and pulsation artefacts using BLADE sequence in knee MR imaging. *Magn Reson Imaging* 2012;**30**(8):1099–110.
14. Nyberg E, Sandhu GS, Jesberger J, *et al*. Comparison of brain MR images at 1.5T using BLADE and rectilinear techniques for patients who move during data acquisition. *AJNR Am J Neuroradiol* 2012;**33**(1):77–82.
15. Holmes JH, Beatty PJ, Rowley HA, *et al*. Improved motion correction capabilities for fast spin echo T1 FLAIR propeller using non-Cartesian external calibration data driven parallel imaging. *Magn Reson Med* 2012;**68**(6):1856–65.
16. Rydén H, Berglund J, Norbeck O, *et al*. T1 weighted fat/water separated PROPELLER acquired with dual bandwidths. *Magn Reson Med* 2018;**80**(6):2501–13.
17. Meier-Schroers M, Sprinkart AM, Becker M, *et al*. Quantitative and qualitative assessment of pulmonary emphysema with T2-weighted PROPELLER MRI in a high-risk population compared to low-dose CT. *Rofo* 2018;**190**(8):733–9.
18. Ohlmann-Knafo S, Morlo M, Tarnoki DL, *et al*. Comparison of image quality characteristics on Silent MR versus conventional MR imaging of brain lesions at 3 Tesla. *Br J Radiol* 2016;**89**(1067):20150801.
19. Zeger SL, Liang KY, Albert PS. Models for longitudinal data: a generalized estimating equation approach. *Biometrics* 1988;**44**(4):1049–60.
20. Alibek S, Adamietz B, Cavallaro A, *et al*. Contrast-enhanced T1-weighted fluid- attenuated inversion-recovery BLADE magnetic resonance imaging of the brain: an alternative to spin-echo technique for detection of brain lesions in the unsedated pediatric patient? *Acad Radiol* 2008;**15**(8):986–95.
21. Pipe JG. Motion correction with PROPELLER MRI: application to head motion and free-breathing cardiac imaging. *Magn Reson Med* 1999;**42**(5):963–9.
22. Hirokawa Y, Isoda H, Maetani YS, *et al*. Evaluation of motion correction effect and image quality with the periodically rotated overlapping parallel lines with enhanced reconstruction (PROPELLER) (BLADE) and parallel imaging acquisition technique in the upper abdomen. *J Magn Reson Imaging* 2008;**28**(4):957–62.
23. Yoneyama M, Nakamura M, Obara M, *et al*. Hyperecho PROPELLER-MRI: application to rapid high-resolution motion-insensitive T2-weighted black-blood imaging of the carotid arterial vessel wall and plaque. *J Magn Reson Imaging* 2017;**45**(2):515–24.
24. Mavroidis P, Giankou E, Tsikrika A, *et al*. Brain imaging: comparison of T1W FLAIR BLADE with conventional T1W SE. *Magn Reson Imaging* 2017;**37**:234–42.
25. Lavdas E, Mavroidis P, Vassiou K, *et al*. Elimination of chemical shift artefacts of thoracic spine with contrast-enhanced FLAIR imaging with fat suppression at 3.0. *Magn Reson Imaging* 2010;**28**(10):1535–40.
26. Shimamoto H, Tsujimoto T, Kakimoto N, *et al*. Effectiveness of the periodically rotated overlapping parallel lines with enhanced reconstruction (PROPELLER) technique for reducing motion artefacts caused by mandibular movements on fat- suppressed T2-weighted magnetic resonance (MR) images. *Magn Reson Imaging* 2018;**54**:1–7.